

# Sliding wear of Cr–Al<sub>2</sub>O<sub>3</sub>–ZrO<sub>2</sub> and Mo–Al<sub>2</sub>O<sub>3</sub>–ZrO<sub>2</sub> composites

S. Scheppokat<sup>a</sup>, R. Hannink<sup>b</sup>, R. Janssen<sup>c</sup>, G. de Portu<sup>d,\*</sup>, N. Claussen<sup>c</sup>

<sup>a</sup> Materials Engineering Hamburg GmbH, Nartenstr. 4a, 21079 Hamburg, Germany

<sup>b</sup> CSIRO Manufacturing and Infrastructure Technology, Private Bag 33, Clayton South, Vic. 3169, Australia

<sup>c</sup> Technical University Hamburg-Harburg, Advanced Ceramics Group, Denickestr. 15, 21073 Hamburg, Germany

<sup>d</sup> Institute of Science and Technology for Ceramics (ISTEC-CNR) via Granarolo, 64; 48018 Faenza (RA), Italy

Received 19 November 2003; received in revised form 4 March 2004; accepted 13 March 2004

Available online 20 June 2004

## Abstract

The sliding wear behavior of a number of reactively sintered metal–alumina-composites (s-MAC) containing zirconia and pure alumina and yttria-stabilized zirconia (3Y-TZP) reference materials were investigated using a ball-on-disk method. Samples were tested against stainless steel (s/steel) and 3Y-TZP ball-sliders. Two series of tests were performed, firstly the samples were tested at low loads against both ball materials and in the second series, the Cr containing composites were tested against the s/steel sliders using increased loads. At low loads, tests against s/steel balls showed no significant differences between samples containing Cr when compared to samples containing Mo. Cr-bearing composites tested against 3Y-TZP showed lowest specific wear rate for this combination of couples. At the low loads no clear correlation was found between hardness and specific wear rate. One Cr containing material showed significantly lower wear than 3Y-TZP, even though it had a slightly lower hardness. Specific wear rates for 3Y-TZP slider balls were significantly higher than for s/steel balls, regardless of the disk material. At high loads, s/steel ball-metal transfer to the specimen disk becomes the dominant “wear” mechanism. This phenomenon occurred to such an extent that the specific wear determined for the sample disks was negative.

© 2004 Elsevier Ltd. All rights reserved.

**Keywords:** Wear; Composites; Al<sub>2</sub>O<sub>3</sub>–ZrO<sub>2</sub>–Cr; Al<sub>2</sub>O<sub>3</sub>–ZrO<sub>2</sub>–Mo; Hardness

## 1. Introduction

Alumina ceramics show excellent sliding wear resistance due to their high hardness. However, the potential of alumina ceramics in many applications is limited by their relatively low toughness. Under wear conditions with high Hertzian contact stresses and cyclic loads, such as in roller bearings, the risk of catastrophic failure, surface fatigue and crack formation are more important than abrasive wear. Under such conditions, a tougher and stronger material can be expected to perform better, as is indicated by the predominant choice of silicon nitride where a ceramic material is used for high speed, high load bearing applications.<sup>1</sup>

One possible way to further improve the toughness of alumina ceramics is the addition of a metal phase. Metal–ceramic composites are promising for a variety of applications. Ideally, they can combine the good properties

of both classes of materials, i.e. the hardness and wear resistance of ceramics with the toughness and damage tolerance of metals. The composites used in this investigation seek to exploit these benefits and were made by a reactive sintering process. The technique used, called the s-MAC (sintered metal–alumina–ceramic composites) process, is derived from the s-3A (sintered alumina–aluminide alloys) process. In the s-3A process, a precursor containing Al<sub>2</sub>O<sub>3</sub>, Al and the oxide of another metal, e.g. TiO<sub>2</sub> or Fe<sub>2</sub>O<sub>3</sub>, is converted to a composite consisting of aluminides and alumina by a redox reaction between aluminum and the metal oxide.<sup>2–7</sup> Because these redox reactions are usually highly exothermic, careful process control is required in order to avoid thermal runaway with possible detrimental effects on the product. In contrast to this, s-MAC precursors consist of Al<sub>2</sub>O<sub>3</sub>, a metal powder such as Cr, Mo, or Fe, and only a small fraction, typically <1 wt.%, of Al. In this case, the redox reaction takes place only on a microscopic scale between Al and the native oxide layer on the particles of the other metal. This has the advantage that no strong exothermic effect occurs during firing and the process is, therefore, easier to control.

\* Corresponding author. Tel.: +39-0546-699752;

fax: +39-0546-46381.

E-mail address: [deportu@istec.cnr.it](mailto:deportu@istec.cnr.it) (G. de Portu).

As with other alumina-based composites, zirconia additions help prevent grain growth and improve the mechanical properties of the final material. This is particularly of interest in the case of Mo–Al<sub>2</sub>O<sub>3</sub> composites, in which the metal phase has grain sizes between 1 and 5 µm and is, therefore, not sufficiently finely dispersed to ensure prevention of excessive grain growth of the alumina at the required sintering temperatures between 1650 and 1700 °C.

It has been demonstrated that the sliding wear resistance of alumina can be further improved by zirconia additions.<sup>8–10</sup> In particular, the load at which a transition from mild to severe wear occurs can be increased.<sup>11</sup> As such a transition increases the specific wear rate of alumina by over two orders of magnitude,<sup>12</sup> this has a very strong effect on the wear behavior. One possible explanation for the improved wear behavior of alumina with zirconia additions is the prevention of grain growth. In most cases, a finer grain size of alumina leads to lower specific wear rates.<sup>13,14</sup> However, this phenomenon appears to be highly dependent on test configuration, as is indicated by other data showing a decrease in specific wear rate with increasing grain size.<sup>15</sup>

Choosing a reactive sintering route for metal–ceramic composites has the advantage that the materials can be sintered pressureless to high densities. It has been shown that materials with 50 vol.% Cr can be sintered to a density of 95% T.D.<sup>16</sup> Even higher densities are achieved for composites with lower metal contents.

It must be pointed out that the investigations described here were aimed at obtaining a number of results for ranking a range of new materials. Therefore, the aim of this study is to present our preliminary observations and hence lacks depth and detail, in particular concerning possible wear mechanisms, and there is clearly a need for more detailed investigations using a broader range of experimental conditions (including longer sliding distance).

## 2. Experimental

Generally, starting powders used in this investigation were attrition-milled 7 h at 700–900 rpm in acetone, using Y-TZP (yttria-tetragonal zirconia polycrystals) milling discs and 3 mm Y-TZP mill media. Materials M10Z10, M20Z16, C10Z10, and C20Z16 were milled in 1 kg batches in a larger attrition mill in ethanol. The starting materials are listed in Table 1, while batch compositions of precursor powders are given in Table 2. The amount of added Al was

Table 2

Batch compositions (wt.%) of precursor powders

	C10Z10	C20Z16	M10Z10	M20Z16	M30Z14
Al <sub>2</sub> O <sub>3</sub>	70.4	51.1	65.7	45.0	35.7
ZrO <sub>2</sub>	13.5	19.6	12.6	17.7	13.7
Cr	15.8	28.7	0	0	0
Mo	0	0	21.3	36.6	49.6
Al	0.3	0.6	0.4	0.7	1.0

calculated to be 2 wt.% of the metal. Calculated compositions of the final materials are given in the sample names: C stands for Cr, M for Mo, and Z for ZrO<sub>2</sub>. The volume percentage of each phase, except alumina, is given after the letter denominating the phase, e.g. C20Z16 is a composite consisting of Al<sub>2</sub>O<sub>3</sub> with 20 vol.% Cr and 16 vol.% ZrO<sub>2</sub>. Al is not considered in the final compositions because at present it is not known which phases are formed during sintering by the initially added Al component. It is known from similar powder-materials processes involving intensive attrition milling that over 50% of the Al initially added can be hydrolyzed or oxidized during milling,<sup>17</sup> so that the remaining amount is in the range of 0.2–0.5 wt.% of the final materials made here and is, therefore, difficult to detect.

The milled slurries were dried overnight and then sieved through a 200 µm screen. Composite samples were compacted by uniaxial pressing at 50 MPa and subsequent isostatic pressing at 900 MPa. Pure alumina (Taimei TM-DAR) and pure zirconia (Tosoh TZ3Y) samples were made by uniaxial pressing at 50 MPa and isostatic pressing at 300 MPa, followed by sintering at 1450 °C for 2 h in air. Sintering of the metal–ceramic composites was done in a graphite lined furnace using the following heating cycle: 10 °C/min → *T*<sub>sinter</sub>, 1.5 h hold, 10 °C/min → RT. The sintering temperature was 1500 °C for samples containing Cr, 1650 °C for samples with 10–20% Mo, and 1700 °C for samples containing 30% Mo. The samples were heated in vacuum up to 400 °C, then 1 bar argon pressure was applied. With one exception, M30Z14, which was post-HIPed in argon for 20 min at 200 MPa and 1550 °C, all materials investigated in this study were sintered pressureless.

The composites can be densified without pressure as the Al reduces any native oxide layer on the metal thereby assists sintering. Fired densities vary with metal content, with typical values of 98% T.D. for composites with 10 vol.% metal and 94–95% T.D. for materials with 20 vol.% metal. The metal phase is homogeneously distributed and does not

Table 1  
Starting materials

Material	Al <sub>2</sub> O <sub>3</sub>	ZrO <sub>2</sub>	Al	Cr	Mo
Manufacturer (type)	Condea Chemie, Brunsbüttel, Germany (HPA 0.5)	Tosoh Corporation, Japan (TZ3Y)	Eckart-Werke, Germany (AS 081)	Alfa Aesar Johnson Matthey, Karlsruhe, Germany	Alfa Aesar Johnson Matthey, Karlsruhe, Germany
Particle size (µm)	0.5	0.28	<45	APS 3–7	APS <10

form a 3D interconnecting network unless the metal content exceeds 30 vol.%, 3Y-TZP additions proved to favor the densification to a small extent. Note that all metal containing samples discussed here were isostatically pressed at 900 MPa in order to obtain high densities and hence good green-state machinability. However, the effect of isostatic compaction pressure on the final sinter density was found to be small, e.g. samples pressed at 300 MPa achieved almost the same density of samples pressed at 900 MPa.

Sintered samples were machined flat and polished to a 3  $\mu\text{m}$  surface finish using a diamond suspension prior to wear testing. Microstructures were observed using a LEO 1540 and a Leica Stereoscan SEM.

The wear behavior of the prepared surfaces was tested, under unlubricated conditions at ambient temperature and humidity, using a ball-on-disk machine designed and built by the CSIRO (effectively a lathe on-end with an instrumented slider arm). The ball sliders comprised carefully selected, commercially available, 10 mm diameter 3Y-TZP grinding media and St316 martensitic-stainless steel (s/steel) ball bearings. In the first series of tests the conditions entailed a normal load of 6.34 N, a sliding speed of 0.75  $\text{m s}^{-1}$  and a total sliding distance of 1000 m; while in the second series, loads of 20 and 60 N were employed to Cr containing composites using the same speed and distance and unlubricated condition. Friction coefficients were recorded throughout the tests, and the equilibrium value after a run-in distance of 500 m was recorded. Before and after testing, samples were ultrasonically cleaned in ethanol and weighed to determine the weight change (loss or gain) using an electronic balance sensitive to four significant places. Determination of sample weight was repeated five times per sample and the average value recorded as the result. The values of the volume loss were obtained dividing  $\Delta P$  by the density. The number of tests for each coupling ranged from one to three.

In order to investigate a possible correlation between hardness and wear behavior, hardness values were measured using a Vickers indenter at load of 98.1 N. The indentation technique was also used to determine the fracture toughness according to the method of Evan and Charles.<sup>18</sup>

### 3. Results and discussion

#### 3.1. Wear tests at 6.34 N load

Microstructural examination of s-MAC materials in the SEM shows that the metal phase has a typical grain size of 1–5  $\mu\text{m}$ . In the matrix, chromium particles generally exhibit more isotropic shape with grain sizes of 1–3  $\mu\text{m}$  (Fig. 1a and b) while molybdenum metal particles are typically elongated and have grain sizes up to 5  $\mu\text{m}$  in length (Fig. 2).

Fig. 3 presents the results of the ball-on-disk wear tests using s/steel and 3Y-TZP balls. It can be noted that in some cases, a specific wear rate of “zero” is indicated; this is because the measuring balance used to determine the weight

change was not, within experimental error, sensitive enough to indicate a detectable weight change, even when a slight wear track was observable on the disk surface and the slider exhibited a significant wear flat. In addition the sliding distance of 1000 m, in some cases, can be considered too short in order to obtain a detectable specific wear rate. However, it was chosen to continue to use the gravimetric method for all investigated samples as alternative suitable approaches, such a volume loss method have their own limitations.<sup>19</sup> The zero weight change result could also be explained as arising from the measured sum of disk mass being equal to the disk mass (wear) loss plus the material transfer from the ball onto the disk. In the later experiments, using higher loads, this transfer resulted in a weight increase, see below.

The 3Y-TZP and alumina reference disk-materials, showed higher specific wear rates against 3Y-TZP balls compared with s/steel balls, see Fig. 3. While the alumina disk showed no measurable wear when tested against s/steel, the 3Y-TZP disk exhibited a specific wear rate of  $62 \times 10^{-6} \text{ mm}^3 \text{ N}^{-1} \text{ m}^{-1}$  and when testing 3Y-TZP balls against 3Y-TZP disks an even higher specific wear rate ( $170 \times 10^{-6} \text{ mm}^3 \text{ N}^{-1} \text{ m}^{-1}$ ) resulted, while the measurable specific wear rate for the pure alumina disk was  $10 \times 10^{-6} \text{ mm}^3 \text{ N}^{-1} \text{ m}^{-1}$ . In all circumstances, the 3Y-TZP disk material showed a higher specific wear rate than alumina.

Significant differences between composites containing chromium and composites containing molybdenum were not observed when tested against s/steel balls. This was different for tests using 3Y-TZP balls, where Cr-bearing samples showed specific wear rate one order of magnitude below M10Z10 and M30Z14. However, M20Z16 was an exception, as this material showed no measurable wear against 3Y-TZP under the chosen test conditions. No measurable wear was also found for M10Z10 against steel balls. It is interesting to note that Cr-bearing samples show lower specific wear rate against 3Y-TZP balls than against s/steel balls (Fig. 3) while they showed lower and higher specific wear rate than the pure alumina disk tested against 3Y-TZP and s/steel, respectively.

All the disks always wear less than the mated 3Y-TZP balls (see Figs. 3 and 6), suggesting consistent material transfer from the ball sliders to the disks. When s/steel balls were used, in some cases (3Y-TZP, M20Z16 and M30Z14), this behavior was not observed. However, when Mo-based composites were rubbed against s/steel, the specific wear rate increased with metal content.

Examination of wear tracks in the SEM showed material transfer from the ball onto the disk as well as surface fracture and pull-out, examples for C10Z10 are shown in Fig. 4(a) and (b). The wear track of C10Z10 against s/steel is shown in Fig. 4(a). In the upper region of the micrograph, surface pull out of the disk is visible as well as dense, light areas which have been identified by elemental mapping as stainless-steel. The wear track in Fig. 4(b) shows even more pronounced material transfer from the ball to the disk in the case of a

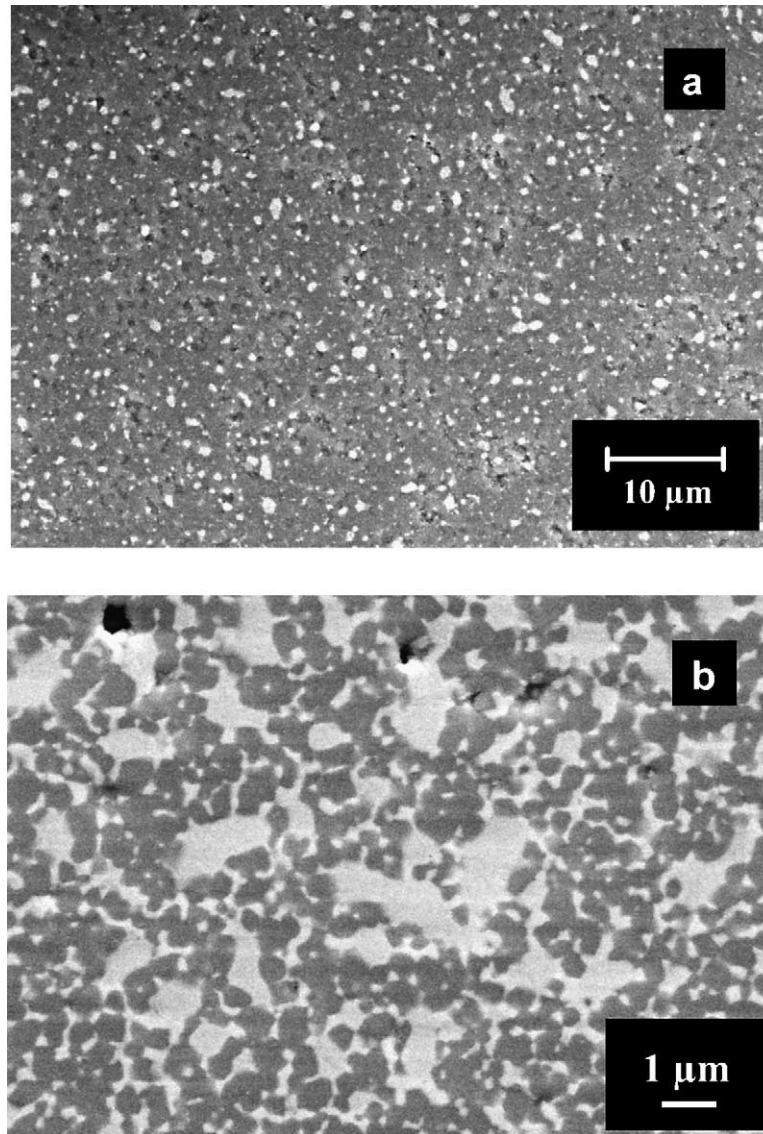


Fig. 1. SEM micrograph of composites: (a) C10Z10 and (b) C20Z16, polished surface. Light phases contain Cr and  $\text{ZrO}_2$ , dark phase  $\text{Al}_2\text{O}_3$ .

3Y-TZP ball. The dense light phase on the left side has been identified as TZP.

The results of the hardness values and indentation fracture toughness, measured using a Vickers indenter, are given in Table 3. As expected, hardness decreases with increasing matrix–metal content. Chromium-bearing samples show slightly higher hardness than comparable materials with molybdenum.

There appeared to be no clear correlation between hardness and specific wear rate for the tests conducted here. Nev-

ertheless it must be noted that M30Z14, the material with the lowest hardness, shows the highest specific wear rate of all tested metal–ceramic composites both against 3Y-TZP and steel balls (Fig. 3). However, while no definitive correlation between hardness and wear behavior could be clearly established, some comment is warranted. The bar graphs plotted in Fig. 3 appear to suggest that against both slider materials, specimen specific wear rate for Cr decrease marginally while for Mo increase marginally, disregarding M20Z16, with increasing matrix–metal contents (Fig. 3). It can be also noted

Table 3  
Vickers hardness ( $H_V$ ) and indentation fracture toughness ( $K_{IC}$ ) of selected metal–ceramic composites and the reference materials

Material	3Y-TZP	$\text{Al}_2\text{O}_3$	C10Z10	C20Z16	M10Z10	M20Z16	M30Z14
$H_V$ (GPa)	12.2	16.7	14.5	11.2	13.3	10.8	9.3
$K_{IC}$ ( $\text{MPa m}^{1/2}$ )	4.3	3.9	7.1	5.8	6.2	8.1	9.9

$H_V$  was measured at a load of 9.8 N.



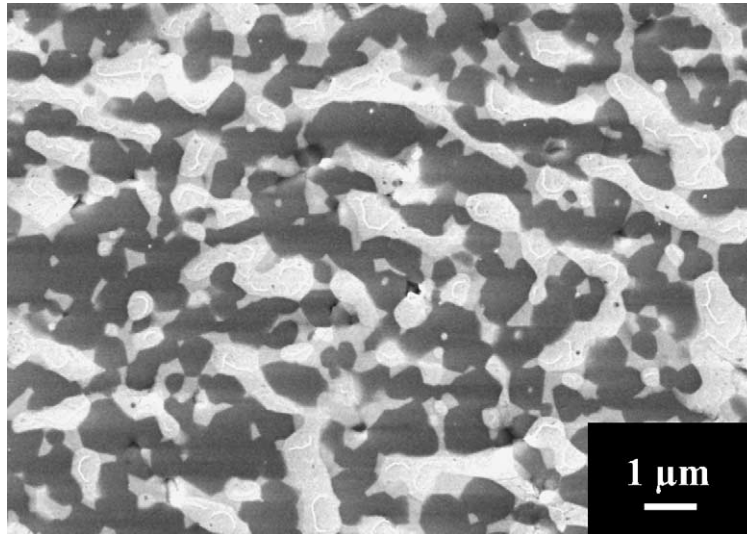


Fig. 2. SEM micrograph of M30Z14, polished surface. Bright phase Mo, grey phase  $ZrO_2$ , and dark phase  $Al_2O_3$ .

that while with the s/steel slider, the coefficient of friction decreases for both matrix–metal systems, it decreases or remains almost constant, respectively, for Cr and Mo, with 3Y-TZP (Fig. 5). The decrease in specific wear rate and in friction for Cr-materials is most likely due to increase slider pick-up to the specimen surfaces. The pick-up effect is more dramatically described in the Section 3.2.

The friction coefficients couples, using 6.34 N slider loads, showed very limited correlation to either type or metal-phase content (see Fig. 5). The friction coefficient against s/steel balls decreases slightly with increasing sample metal content, while values for the ceramic reference materials, without metal, showed lower or equal friction. In all instances, the metal–ceramic composites showed higher friction coefficients against s/steel sliders than against 3Y-TZP. This difference was largest in the case of C20Z16, which exhibited, for a 6.34 N load, an equilibrium friction coefficient of 0.50 against 3Y-TZP and 0.93 against s/steel. Pure 3Y-TZP disks showed no significant differences in

friction coefficient for both slider materials. For alumina, the friction coefficient was, in the light load regime, higher against s/steel balls, 0.83, which is in turn higher than previously reported literature values.<sup>20</sup> Friction of alumina against s/steel has been found to depend significantly on speed, for the speed used in this study, values of approximately 0.50 have been reported.<sup>20</sup>

When the friction coefficient data obtained in this study, as a function of speed and loads are compared to those previously reported for similar testing conditions, the values measured in this study as a function of speed and loads are, in some cases, different or consistent. For example in the case of SiC disk and 7 wt.% Co–WC slider couples<sup>19</sup> the friction coefficient is higher (about 1.2). On the contrary when  $Al_2O_3$  and  $Al_2O_3 + Mo$  disks are used by de Portu et al.<sup>21</sup> the values of  $\mu$  are similar to those measured here.

Notwithstanding our agreement with the work of de Portu et al.<sup>21</sup> in general, friction coefficients vary considerably and are highly dependant on test couple and parameters.

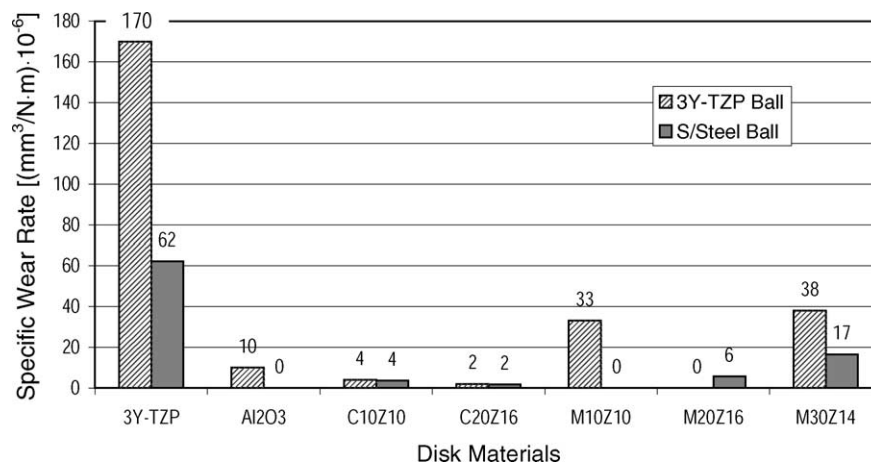


Fig. 3. Specific wear rate of different disk materials against steel and 3Y-TZP balls.

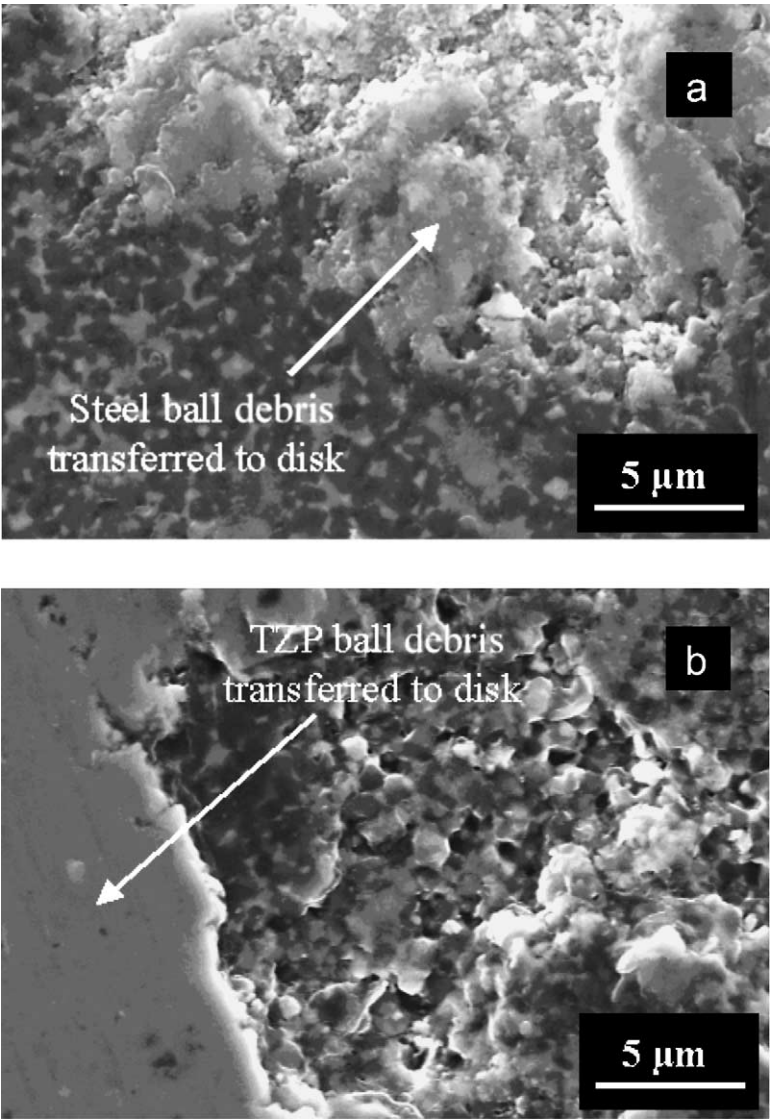


Fig. 4. SEM micrographs of wear tracks on C10Z10 against (a) steel ball and (b) 3Y-TZP ball.

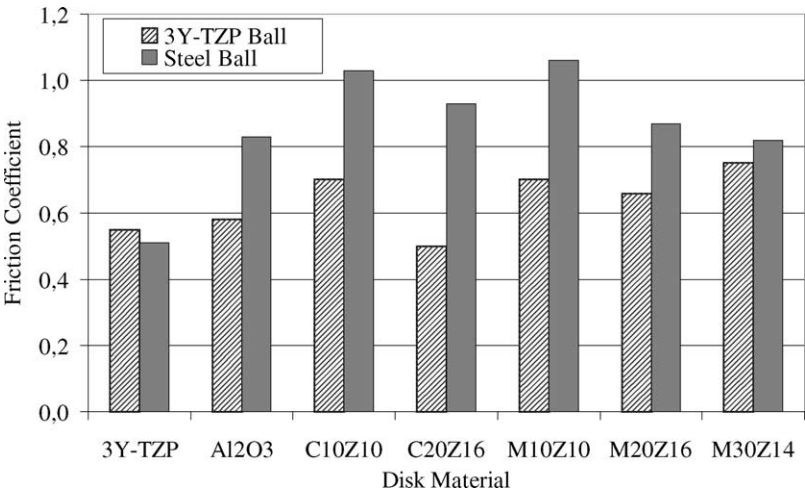


Fig. 5. Friction coefficients of different disk/ball couplings at normal load of 6.34 N.

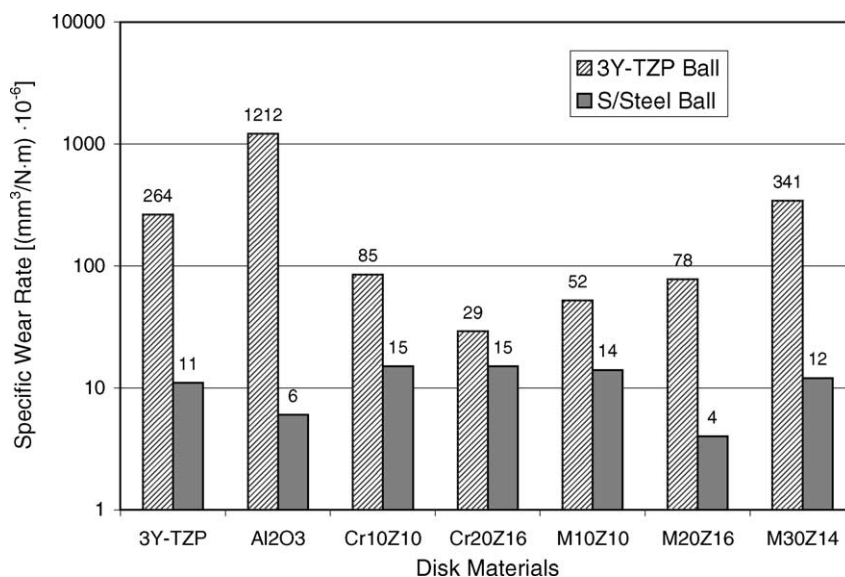


Fig. 6. Specific wear rate of s/steel and 3Y-TZP ball-sliders against the different disk materials.

Previous studies between ZTA disks and alumina spheres have yielded friction coefficients between 0.45 and 0.55 in one study,<sup>8</sup> values  $<0.2$  have been found for alumina spheres on zirconia in another work.<sup>10</sup> For alumina/alumina couples, values around 0.9 have been reported.<sup>13</sup> Thus, a consistent friction coefficient for metal–ceramic/ceramic or ceramic/ceramic couples has not been established and reported to the knowledge of these authors.

Since wear is also a test system-configuration property, it is important to include results of the wear behavior of the opposing partner in all discussions. Fig. 6 shows the wear behavior of s/steel and 3Y-TZP balls against the different test-disks. The specific wear rate of the s/steel balls is of the same order against all tested disk materials. For 3Y-TZP balls, the variation is larger, with values differing by more than an order of magnitude. What may be of significance is that, in all cases, s/steel balls show substantially lower specific wear than 3Y-TZP balls. The largest difference in slider wear behavior was that observed for 3Y-TZP against Al<sub>2</sub>O<sub>3</sub> and against M30Z14, where the values for s/steel and of 3Y-TZP slider wear differ by about two orders of magnitude. In other cases, ball specific wear was less pronounced, e.g. for C20Z16, both slider materials showed specific wear rate of the same order.

Self-mated TZP shows, approximately, similar wear for both disk and ball. However, when mated with the other materials, TZP sliders always show a higher specific wear rate (often even one order of magnitude higher) than the disks. This is the consequence of the massive material transfer observed from the ball to the disk. For Cr based composites, the specific wear rate of TZP sliders decreases with increasing the metal content while for the Mo composites it increases.

The slider wear comparison between s/steel and 3Y-TZP is particularly interesting because both materials have similar elastic moduli, so that initial contact stresses are com-

parable. The comparison between steel and 3Y-TZP leads to the conclusion that system wear (ball + disk) is substantially lower for hybrid systems “ceramic against steel” for the cases investigated here. This observation leads to the further speculation regarding wear behavior, which includes variables such as thermal conductivity and effects of materials transfer.

### 3.2. Wear tests at 6.34, 20, and 60 N loads

In an effort to increase wear and to determine the effect of load, on a couple which in general was the best performing system studied here, viz. Cr10Z10 and Cr20Z16 with s/steel sliders, additional tests were performed at 20 and 60 N slider loads. It was felt that this s-MAC system coupled to stainless steel was also the most likely to find industrial application, in for example pumps and sliding automotive conditions hence the attempt to simulate extreme industrial conditions.

The results obtained were somewhat unexpected and are shown in Figs. 7 and 8. Fig. 7 shows the specific wear rate of the two Cr compositions against the s/steel slider, indicates that the wear is reducing as a function of load and in fact, it converges to similar negative values for the 60 N load. The Cr20Z16 sample, i.e. the lowest hardness but highest matrix metal content, showed the lowest specific wear rate, at the lower load. Correspondingly, the specific wear rate of the s/steel ball slider (Fig. 8) as a function of load, is highest for the C20Zr16 sample.

The results as a function of load appear to indicate unequivocally that, for zirconia containing s-M(Cr)AC, wear against s/steel is a balance between sample surface loss and slider material transfer, and as load is increased for our system, the slider metal-transfer dominates.

The observations as a function of increased load may well indicate that it is very difficult to compare s-MAC and

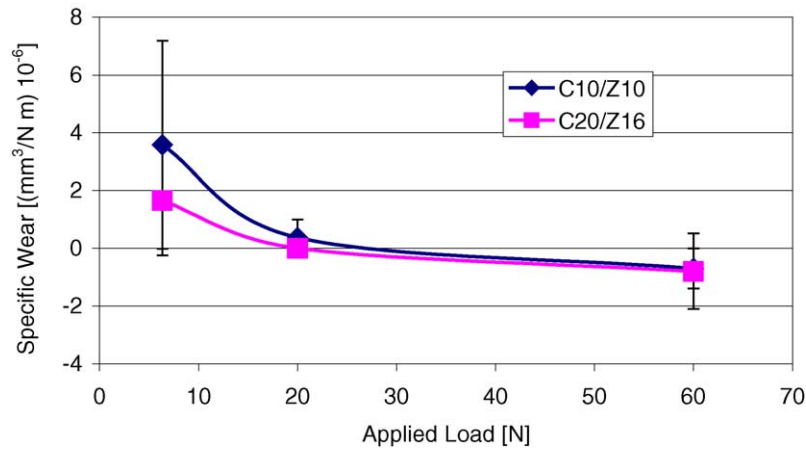


Fig. 7. C10Z10 and C20Z16 disk specific wear rate as a function of s/steel slider-arm load.

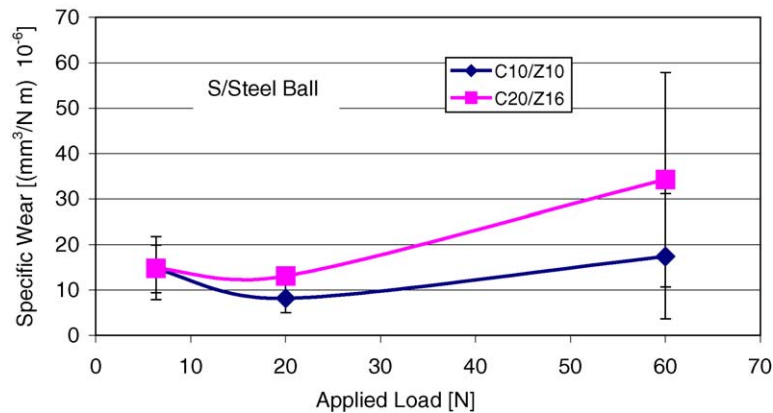


Fig. 8. Stainless steel slider ball specific wear rate against C10Z10 and C20Z16 as a function of slider arm-load.

pure ceramic systems against metal, s/steel in this case, as the wear mechanisms are inherently different.<sup>22</sup> Stachowiak and Stachowiak<sup>22</sup> studies ceramic disc and metal pin wear systems. Even though their conditions were much milder than those used here,  $0.08 \text{ m s}^{-1}$  sliding velocity and  $3.7 \text{ N}$  normal load, they concluded that in all cases metal–ceramic sliding contact was associated with metal transfer onto the ceramic disc and that direct metal–metal contact then controlled the friction and wear behavior of the sliding pair.

For the systems examined here as a function of load, the more matrix–metal present, the greater the “stick-slip” transfer from the slider and a significantly lower specimen disk loss occurring as a function of fatigue-breakout, resulting in an overall specimen mass gain, while for the pure ceramic–metal sliding, i.e. alumina and 3Y-TZP, wear is controlled by the modulus ( $E$ ) and the hardness ( $H_V$ ) of the disc material. In this case, the ceramic modulus will control the contact fatigue ( $E \sim 2\times$  higher for alumina than 3Y-TZP) and hardness ( $H_V$  about 30% higher for alumina than 3Y-TZP, see Table 3). Very little wear correlation could be made with the indentation fracture toughness. During the test process, the s/steel slider wears by work hardening-micro-machining, while the specimen

disk, when occurring, appears to wear by surface fatigue and pull-out. Therefore, under these test conditions, sliding against s/steel, alumina is far more resistant to surface fatigue and has a hardness advantage over 3Y-TZP.

#### 4. Conclusions

The results for slider ball-on-disk wear tests of metal–ceramic composite (s-MAC), with zirconia, performed in this study have shown that it is difficult to establish well-defined relationships between composition, test configuration, and wear properties. However, a number of conclusions can be made based on the results obtained:

- The specific wear rate of most slider metal–ceramic composites vary by only one order of magnitude.
- One tested material, C20Z16, showed specific wear rate more than an order of magnitude lower than the 3Y-TZP reference disk, although it has a slightly lower hardness than 3Y-TZP. This was the case both against s/steel and against 3Y-TZP balls.



- Stainless steel slider-balls show lower specific wear rate than 3Y-TZP slider-balls against all tested disk materials, suggesting that thermal conductivity is a parameter that warrants further investigation.
- There is no clear correlation between disk metal content, hardness and specific wear rate under the chosen test conditions, this may have partly been due to the transfer of slider ball-materials to the sample disk.
- The results indicated that the disc wear was lower for hybrid systems “metal–ceramic composite against s/steel,” when, particularly at higher loads, true disk specific wear rates were often masked by slider-metal transfer to the disk surface such that a very low or negative specific wear rate of disk resulted.
- For the limited examples observed, it appeared that the s-MAC sample wear mechanism is one related to surface fatigue and brittle macro-fracture rather than micro-breakout or machining.
- A further study is necessary to identify the parameters most important for true disc wear rather than metal pick-up. Among these parameters, hardness and couple-thermal conductivity deserve more consideration and further study, while additional parameters such as slider materials may also need to be optimized to permit further study of the metal–ceramic disk wear mechanism.

## Acknowledgements

The authors gratefully acknowledge the generous financial support from NEDO (New Energy and Industrial Technology Development Organization), Japan and CNR-CSIRO International Scientific Cooperation Agreement, Joint Research Project, without which this study would not have been possible. The authors also take pleasure in acknowledging the students, Christian Rottmeier, Stefan Rau, and Petra Bartels, whose technical assistance has been invaluable in operating the equipment and collecting the experimental data.

## References

- Richerson, D. W., *Modern Ceramic Engineering*. Marcel Dekker, New York, 1992, ISBN 0-8247-8634-3.
- Claussen, N., Garcia, D. E. and Janssen, R., Reaction sintering of alumina–aluminide alloys (3A). *J. Mater. Res.* 1996, **11**(11), 2884–2888.
- Schicker, S., Erny, T., Garcia, D. E., Janssen, R. and Claussen, N., Microstructure and mechanical properties of Al-assisted sintered Fe/Al<sub>2</sub>O<sub>3</sub> cermets. *J. Eur. Ceram. Soc.* 1999, **19**(13/14), 2455–2463.
- Schicker, S., Garcia, D. E., Bruhn, J., Janssen, R. and Claussen, N., Reaction processing of Al<sub>2</sub>O<sub>3</sub> composites containing iron and iron aluminides. *J. Am. Ceram. Soc.* 1997, **80**(9), 2294–2300.
- Garcia, D. E., Schicker, S., Bruhn, J., Janssen, R. and Claussen, N., Synthesis of novel niobium aluminide-based composites. *J. Am. Ceram. Soc.* 1997, **80**(9), 2248–2252.
- Gaus, S. P., Harmer, M. P., Chan, H. M., Caram, H. S. and Claussen, N., Alumina–aluminide alloys (3A) technology. Pt. 1: Model development. *J. Am. Ceram. Soc.* 2000, **83**(7), 1599–1605.
- Gaus, S. P., Harmer, M. P., Chan, H. M., Caram, H. S., Bruhn, J. and Claussen, N., Alumina–aluminide alloys (3A) technology. Pt. 2: Modelling of Ti<sub>x</sub>Al<sub>y</sub>–Al<sub>2</sub>O<sub>3</sub> composites formation. *J. Am. Ceram. Soc.* 2000, **83**(7), 1606–1612.
- Kerkwijk, B., Winnubst, L., Mulder, E. J. and Verweij, H., Processing of homogeneous zirconia-toughened alumina ceramics with high dry-sliding wear resistance. *J. Am. Ceram. Soc.* 1999, **82**(8), 2087–2093.
- He, Y. J., Winnubst, A. J. A., Schipper, D. J., Burggraaf, A. J. and Verweij, H., Effects of a second phase on the tribological properties of Al<sub>2</sub>O<sub>3</sub> and ZrO<sub>2</sub> ceramics. *Wear* 1997, **210**, 178–187.
- Esposito, L., Moreno, R., Sánchez Herencia, A.J. and Tucci, A., Sliding wear response of an alumina–zirconia system. *J. Eur. Ceram. Soc.* 1998, **18**, 15–22.
- He, C., Wang, Y. S., Wallace, J. S. and Hsu, S. M., Effect of microstructure on the wear transition of zirconia-toughened alumina. *Wear* 1993, **162/164**, 314–321.
- Munro, R. G., Evaluated material properties for a sintered  $\alpha$ -alumina. *J. Am. Ceram. Soc.* 1997, **80**(8), 1919–1928.
- Senda, T., Yasuda, E., Kaji, M. and Bradt, R. C., Effect of grain size on the sliding wear and friction of alumina at elevated temperatures. *J. Am. Ceram. Soc.* 1999, **82**(6), 1505–1511.
- Krell, A. and Klaffke, D., Effects of grain size and humidity on fretting wear in fine-grained alumina, Al<sub>2</sub>O<sub>3</sub>/TiC, and zirconia. *J. Am. Ceram. Soc.* 1996, **79**(5), 1139–1146.
- Xiong, F., Manory, R. R., Ward, L. and Terheci, M., Effect of grain size and test configuration on the wear behavior of alumina. *J. Am. Ceram. Soc.* 1997, **80**(5), 1310–1312.
- Leverkoehne, M., *Fabrication and Characterization of Multifunctional Metal–Ceramic Composites*, Reihe 5, Nr. 637. Fortschritt-Berichte VDI Verlag, 2001, ISBN 3-18-363705-7.
- Holz, D., Wu, S., Scheppokat, S. and Claussen, N., Effect of processing parameters on phase and microstructure evolution in RBAO ceramics. *J. Am. Ceram. Soc.* 1994, **77**(10), 2509–2517.
- Evan, A. G. and Charles, E. A., Fracture toughness determination by indentation. *J. Am. Ceram. Soc.* 1976, **59**(7/8), 371–372.
- Guicciardi, S., Melandri, C., Lucchini, F. and de Portu, G., On data dispersion in pin-on-disk wear tests. *Wear* 2002, **252**, 1001–1006.
- Ravikiran, A., Nagarajan, V. S., Biswas, S. K. and Pramila Bai, B. N., Effect of speed and pressure on dry sliding interaction of alumina against steel. *J. Am. Ceram. Soc.* 1995, **78**(2), 356–364.
- de Portu, G., Guicciardi, S., Melandri, C. and Sbaizero, O., *Wear Behavior of Al<sub>2</sub>O<sub>3</sub>–Mo Composites*, *Ceramics: Getting into the 2000s—Part C: Advances in Science and Technology*, Vol 15, ed. P. Vincenzini. Techna, 1999, pp. 771–778.
- Stachowiak, G. W. and Stachowiak, G. B., Metallic film transfer during metal–ceramic unlubricated sliding. *Wear* 1989, **132**, 361–381.